# Investigation of the extreme-UV background emission in WEST tokamak

M.B. Boumendjel[1], R. Guirlet[1], C. Desgranges[1], J.L. Schwob[2], P. Mandelbaum[3], E. Popov[4], O. Peyrusse[5] and the WEST team[1].

[1] *CEA, IRFM, F-13108 St Paul-lez-Durance, France.*

[2] *Racah Institute of Physics, Jerusalem, Israel*

[3] *Jerusalem College of Engineering, Ramat Beth Hakerem, Jerusalem, Israel*

[4] *Aix-Marseille Université, Institut Fresnel UMR 7249, Marseille, France.*

[5] *Aix-Marseille Université, LP3, Marseille, France*

The inner walls of current (WEST, AUG, JET) and future (ITER) tokamaks use tungsten W. In such a wall configuration, one of the issues is the tungsten effect on plasma fusion performance. Thus it is necessary to monitor W density. Many research works were performed to determine the W density experimentally [1, 2]. However, little attention has been given to the tungsten spectrum background that may affect its density determination. The aim of this work is to analyze the tungsten spectrum background (115-165 Å) measured in the WEST tokamak by a grazing incidence spectrometer [3] (Fig. 1 (a)). The instrument has been calibrated in absolute units of brightness [4]. An example of a spectrum measured on WEST to which a fitting

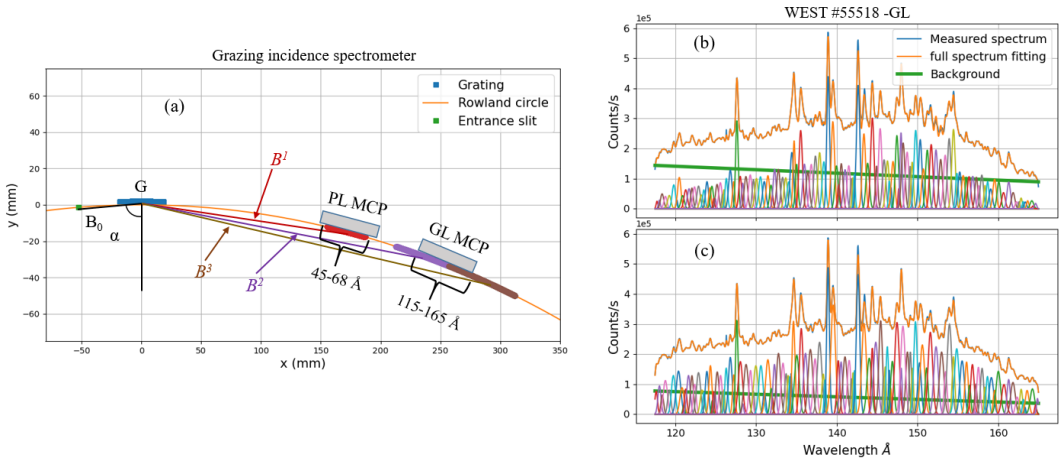


Figure 1: *(a) Absolutely calibrated Grazing Incidence Spectrometer equipped with a 600g/mm concave grating (G) and two multichannel detectors MCP (PL and GL) that scan along the Rowland circle. (b) Example of spectrum measured on WEST and a result of the fitting procedure. (c) Same as (b).*

procedure is applied is shown in Fig. 1 (b) and (c). The fitting method consists of minimizing the difference ($\chi^2$) between the measured spectrum and the model (in which the background is represented by a polynomial and the spectral lines by Gaussian functions). The fitting results (orange color in Fig. 1 (b) and (c)) are very good. However, the background and line amplitude values depend strongly on the initial guesses as can be seen in Fig. 1 (b) and (c), which affect the determined physical quantity (W density in particular). For this reason, it is necessary

to ascertain the physics basis for the spectrum background. This is done by assuming that the measured spectrum brightness $B_{tot}$ is composed of: spectral lines $B_{line}$, Bremsstrahlung $B_{ff}$, recombination radiation $B_{fb}$ and higher diffraction orders emission $B^{m>1}$:

$$B_{tot} = B_{line} + B_{ff} + B_{fb} + B^{m>1} \tag{1}$$

The brightness (Photons cm$^{-2}$ s$^{-1}$ sr$^{-1}$) for the first three terms is defined as the integral of the local emissivity $\varepsilon^z$ along the line of sight: $B = \frac{1}{4\pi}\int \varepsilon^z dl$. The expression of the last term $B^{m>1}$ will be derived below.

**Background emission**

Bremsstrahlung (free-free) and recombination radiation (free-bound) are calculated using the Maxwellian averaged emission coefficients ($C^z_{ff}$ and $C^z_{fb}$) reported in [5]. These coefficients are used because they provide a reasonable and fast estimation of the two processes, which allows us to investigate a broad range of wavelength (10-300 Å) and electron temperature $T_e$ (50-5000 eV). The comparison of Bremsstrahlung and radiative recombination is done for tungsten by calculating the local emissivity ratio $R_\varepsilon$ of the two processes:

$$R_\varepsilon = \frac{\varepsilon_{ff}}{\varepsilon_{fb}} = \frac{n_e N_w \sum_z f_z C^z_{ff}}{n_e N_w \sum_z f_z C^z_{fb}} = \frac{\sum_z f_z C^z_{ff}}{\sum_z f_z C^z_{fb}} \tag{2}$$

The W fractional abundance $f_z$ is calculated with ADAS [6]. The ratio $R_\varepsilon$ is shown in Fig. 2. It can be seen that radiative recombination is negligible with respect to Bremsstrahlung above $\lambda \approx 50$ Å for almost all temperatures. For smaller wavelength, the radiative recombination is not negligible, and can be dominant below $T_e \approx 500$ eV. The total Bremsstrahlung is computed using the expression of the effective charge $Z_{eff}$ [7]:

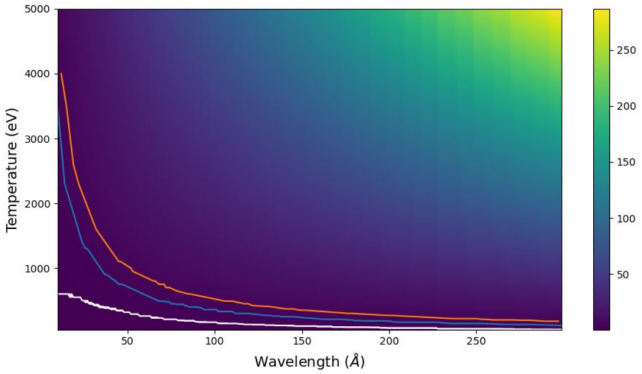


Figure 2: *Emissivity ratio $R_\varepsilon$ as a function of $T_e$ and $\lambda$. White curve: $R_\varepsilon \approx 1$, blue: $R_\varepsilon \approx 3$ and red: $R_\varepsilon \approx 5$.*

$$\varepsilon_{ff}(\lambda) = 9.584.10^{-14} \frac{n_e^2}{\lambda\sqrt{T_e}} Z_{eff} \overline{G_{ff}} \exp(-\frac{hc}{\lambda T_e}) \tag{3}$$

The expression for the last term $B^{m>1}$ in Eq. (1) is derived using the following reasoning: a beam of light, characterised by its brightness $B_0$, hits the grating $G$ with an incidence angle $\alpha = 88.5°$ (see Fig. 1 (a)). The light diffracted in each order m is equal to the brightness $B_0$ multiplied by the grating efficiency of that order $E^m_G$. This quantity is then multiplied by the detector efficiency $E_D$ to obtain the measured brightness $B^m$ at apparent wavelength $m\lambda$:

$$B^m(m\lambda) = B_0\, E_G^m(\lambda)\, E_D(\lambda) \tag{4}$$

the second and third diffraction order of the spectrum measured by PL ($\lambda = 45-68$ Å) may contribute to the spectrum measured by GL ($\lambda = 115-165$ Å), as shown in Fig. 1 (a). Each order contribution can be estimated using Eq. (4):

$$\frac{B^{m>1}(m\lambda)}{B^1(\lambda)} = \frac{E_G^{m>1}(\lambda)}{E_G^1(\lambda)} \frac{E_D^{GL}(\lambda)}{E_D^{PL}(\lambda)} = K^{m>1}(\lambda) \tag{5}$$

Rearranging this equation yields $B^{m>1}(m\lambda)$ as function of the first order spectrum $B^1(\lambda)$:

$$B^{m>1}(m\lambda) = B^1(\lambda) K^{m>1}(\lambda) \tag{6}$$

The coefficient $K^{m>1}(\lambda)$ can be seen as a function that relates the spectrum brightness of a particular order m to the first order spectrum. The grating efficiency $E_G^m$ is calculated using the differential method [8]. The results of the first three orders are shown in Fig. 3 (a). The detectors efficiency ratio is assumed to be a constant close to 1 since they are almost identical. The calculated coefficient $K^{m>1}$ (blue) and the measured one $K^2_{mes}$ [4] (two green points) are given in Fig. 3 (b). The agreement between $K^2$ and $K^2_{mes}$ is good, and the difference between the calculations and the measurements is due to the small variation of $E_D^{GL}/E_D^{PL}$ around 1, and to the concave grating aberrations that can introduce an error up to 15 %. Recently, the detector PL has been damaged and replaced by a similar one, but with an efficiency twice lower than that of GL. Thus, a ratio $E_D^{GL}/E_D^{PL} \approx 2$ will be used in the calculations for spectra measured after this change.

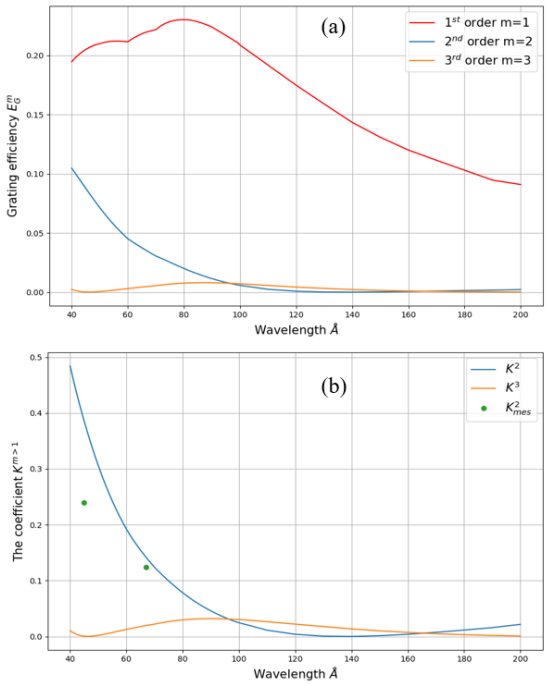


Figure 3: *(a) Grating efficiency. (b) The coefficient* $K^{m>1}$.

## Application

The procedures described previously to calculate the background emission are applied to a spectrum measured by the detector GL (115-165 Å) during the discharge #55647. The maximum density and temperature along the spectrometer line of sight are $n_e = 4.5 \times 10^{13}$ cm$^{-3}$ and $T_e = 1200$ eV, respectively. An effective charge $Z_{eff} = 2.5$ is used to evaluate the total Bremsstrahlung emissivity. Because the two detectors PL and GL cannot measure simultaneously the wavelength regions 45-68 and 115-165 Å due to the dimensions of the two detector

carriages [3], a spectrum measured during the discharge #55589 (see Fig. 4 (a)) is used to estimate the second and third diffraction orders ($B^2$ and $B^3$) of the quasi-continuum (QC) emission around 60 and 50 Å. The spectrum brightness $B_{tot}$ and its background components as defined by Eq. (1) are shown in Fig. 4 (b). The results show that the calculated Bremsstrahlung and third order emission are negligible. However, a careful analysis of the peak positions show that the spectrum above above 145 Å corresponds extremely well with the 47-52 Å QC, which casts some doubt on the calculation of the third order. This now under investigation. The second order emission $B^2$ contributes to the spectrum brightness and it is possible to observe second order spectral lines in the wavelength region 115-135 Å. However, The most significant contribution to the spectrum $B_{tot}$ is the first term $B_{line}$, which indicates that the spectral lines dominate the emission in the wavelength region 115-165 Å at low temperatures ($T_e \approx 1$ keV).

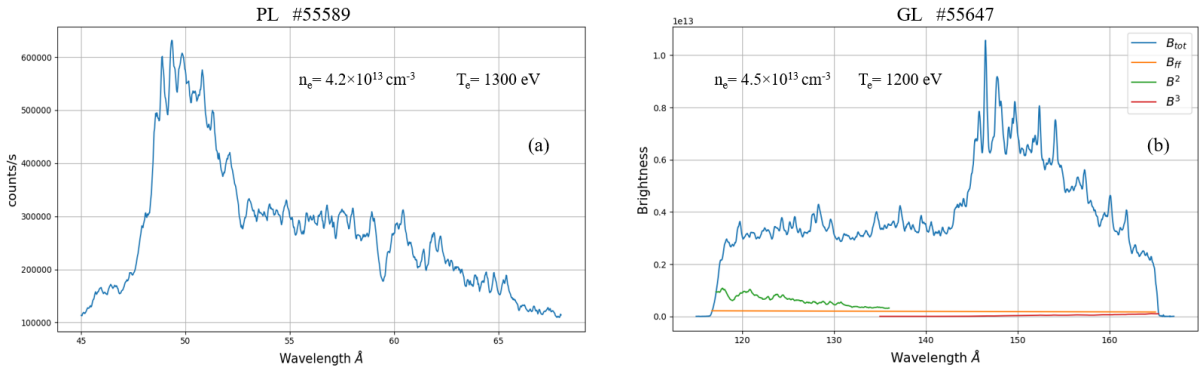


Figure 4: *(a) Quasi-continuum (QC) emission around 50 and 60 Å (#55589). (b) Spectrum brightness (#55647) and its background components.*

**Acknowledgement:** This work has been carried out within the framework of the EUROfusion Consortium, funded by the European Union via the Euratom Research and Training Programme (Grant Agreement No 101052200 — EUROfusion). Views and opinions expressed are however those of the author(s) only and do not necessarily reflect those of the European Union or the European Commission. Neither the European Union nor the European Commission can be held responsible for them.

## References

[1] K. Asmussen, et al. Nuclear fusion 38.7: 967, 1998.

[2] R. Guirlet, et al. Plasma Physics and Controlled Fusion, 2022.

[3] J.L. Schwob, et al. Review of scientific instruments 58.9: 1601-1615, 1987.

[4] R. Guirlet, J.L. Schwob, O. Meyer, and S. Vartanian. Journal of Instrumentation, 12(01), P01006, 2017.

[5] A. Burgess, H.P. Summers, Monthly Notices of the Royal Astronomical Society, 226(2):257–272, 1987.

[6] H.P. Summers, The ADAS User Manual, version 2.6 http://www.adas.ac.uk

[7] M.E. Foord, E.S. Marmar, and J.L. Terry, Review of Scientific Instruments, 53(9), 1407-1409, 1982.

[8] E. Popov, M. Neviere. J. Opt. Soc. Am. A, 18, 2886–2894, 2001.